



# Effective IoT Based Analysis of Photoplethysmography Waveforms for Investigating Arterial Stiffness and Pulse Rate Variability

Srinivasa Rao Sankranti<sup>1</sup> · S. Mahaboob Basha<sup>2</sup> · B. Laxmi Kantha<sup>3</sup> · L. Bhagyalakshmi<sup>4</sup> · N. Gomathi<sup>5</sup> · Kuchipudi Prasanth Kumar<sup>6</sup> · Sanjay Kumar Suman<sup>7</sup>

Received: 8 August 2023 / Accepted: 6 March 2024  
© The Author(s), under exclusive licence to Springer Nature Singapore Pte Ltd. 2024

## Abstract

In order to detect variations in blood volume in the peripheral arterial pulse, photoplethysmography (PPG) can be used as an electro-optical method. Recognized as a straightforward, non-invasive, and reasonably priced method for diagnosing cardiovascular issues, PPG pulse characterization has attracted a lot of attention in recent years. IoT based analysis of PPG contours can shed light on cardiac characteristics at various points in the cardiac cycle. Loss of pulsatility associated with age and Cardio Vascular Disease (CVD) is the primary limitation of contour analysis. The e waves are classified through optimistic discrete wavelet and CNN based approach. As a result, IoT based accurate delineation of the PPG pulse is necessary for accurate detection of heart illness. In addition, resampling the SDPPG signal ensures the occurrence of particular facts when it comes to the process of building slabs of attention, in which the undesired slabs are primarily removed by means of onset criteria. Research provides a comparison of the performance of the proposed method to that of other machine learning based techniques. In terms of classification accuracy (Normal, P1, and P2 pulses: 95.9%, 93.4%, and 90.08% respectively), wavelet-based CNN with PPG signal outperforms CNN with PPG and ABP signals. Correct classification is aided by CNN's ability to extract many features associated with premature pulses. To ensure that no pulses are missed, our method estimates the wavelet transform at one-second intervals over the whole signal's duration. CNN's incremental fine tuning also aids in improving both sensitivity and specificity. The wavelet-based CNN outperforms other state-of-the-art approaches in terms of accuracy, sensitivity, and specificity when classifying waves.

**Keywords** Photoplethysmography (PPG) · Heart rate variability (HRV) · Pulse rate variability (PRV) · Electro cardio gram (ECG) · Cardio vascular disease (CVD) · Internet of things (IoT)

## Introduction

As technology and methods have improved, CVD may now be diagnosed and monitored with greater accuracy and efficiency in the medical system. It is preferable to minimise the hazards associated with surgically accessing the body's surface, such as infection, hence non-invasive approaches have played an important role in biomedical monitoring and diagnosis. Tonometry, echo tracking, Doppler probes, Electrocardiography (ECG), and Photoplethysmography (PPG) are all examples of non-invasive procedures that can be used to evaluate cardiovascular disorders [1, 2].

The optical evaluation of physiological parameters provides circumstances for continuous, non-invasive physiological monitoring, which is the foundation for diagnosis and therapy. Photoplethysmography (PPG) is a photosensitive method applied in virtually every clinical setting because of its ease of use, low cost, and high utility. PPG is able to detect changes in blood volume in the micro vascular bed of tissue by operating in the red or near infrared range (NIR) [3]. The peripheral pulse that coincides with the heartbeat is the most prominent aspect of the waveform. The PPG signal has been widely recognised for its potential to provide insightful cardiovascular data. The development of computer-based pulse wave analysis tools and the technique's attractive simplicity, portability, and low cost have sparked renewed interest in it in recent years [4–6].

---

This article is part of the topical collection “Machine Intelligence and Smart Systems” guest edited by Manish Gupta and Shikha Agrawal.

---

Extended author information available on the last page of the article

With the help of a secure service layer (SSL) and the ability to collect, record, and analyse a new data stream with extreme precision and speed, the Internet of Things (IoT) is a network that connects all the things in our environment to the internet to share and capture the crucial amount of information. The healthcare system's service quality may increase automatically, and costs may decrease, if the philosophy of the Internet of Things (IoT) is applied in this sector. Research efforts have been concentrated on several aspects of healthcare, including monitoring and control, interoperability and security, big data analysis and management, pervasive healthcare and sensing, etc.

The number of people affected by CVD has grown. Arterial stiffness is the primary predictor of cardiovascular risk since it is directly related to the progression of atherosclerosis and arteriosclerosis, an inflammatory and degenerative condition of the arterial wall. Arterial stiffness is a normal part of ageing, but it can be accelerated by conditions including high blood pressure, high cholesterol, and diabetes. Traditional assessment of arterial stiffness has relied on pulse wave velocity (PWV), which is a measure of major artery segments [7].

Although aortic structural abnormalities may be a presenting symptom rather than the underlying cause of cardiovascular disease, studies focusing on smaller arteries are important for early detection of cardiovascular events caused by arterial stiffness. Information about the periphery's arteries can be gleaned from the PPG pulse wave. The forward wave of a PPG pulse travels from the heart to the finger, while the reverse wave travels back through the aorta to the femoral and popliteal arteries in the legs [8–10]. Smaller arteries become stiffer, changing the magnitude and timing of the reflected waves. Therefore, it is necessary to collect the information on vascular stiffness by a promising method, involving the IoT based delineation and analysis of the contour of the PPG pulse wave.

The optical qualities of a chosen skin area constitute the basis for PPG. The epidermis, dermis, and subcutaneous fat are the three main layers of skin that can be seen from the outside. The epidermis, the outermost layer of skin, typically measures 100  $\mu\text{m}$  in thickness, lacks blood vessels, and sheds its dead cells on a regular basis. Capillaries are extremely fine blood channels that transport oxygenated blood from the arteries to the cells that need it (the mitochondria) and waste products (the erythrocytes) to the venules. The subcutaneous tissue is a layer of fatty and connective tissue (1–6 mm thick) that protects the body's major blood arteries and nerves [12–14].

As can be seen in Fig. 1, the PPG waveform is made up of two distinct waves: a great quasi-DC module that associates the tissues and the middling lifeblood volume, and an AC or pulsatile component that synchronises with the heart

rate and is superimposed on the big quasi-DC component. The amplitude of the pulsatile constituent of the PPG data is typically 1–2 percent of the DC value, and it is indicative of vascular compliance and cardiac function. Important data about how blood is pumped and moved around the body of a living organism can be found in its pulsatile component [15]. This has been used to examine peripheral vascular compliance and major artery compliance, making it a valuable tool for the study of cardiovascular disease. In this publication, the pulsating part of PPG is called the PPG pulse wave.

## Motivation for the Research

This investigation seeks to make two contributions to the field of photoplethysmographic cardiovascular assessment. First, it will investigate the arterial stiffness of subjects whose morphology varies (for instance, the data may reveal varying pathophysiological intricacies, such as consistent and uneven heart beats, squat and varying amplitudes). Second, it will investigate the potential of PPG signal to evaluate cardiovascular dynamics. Changes in blood volume in the micro vascular bed of tissues can be detected using PPG, an optical technique that typically operates in the red or near infrared area. Hertzman and Spielman were the first to use the term “photoplethysmography,” and they proposed that the resulting “plethysmogram” quantify changes in blood vessel volume [11].

## Database Applied

The waveforms for PPGs are taken commencing PhysioNet's (<http://www.physionet.org>) massive, freely accessible data record. The database includes high-perseverance physiologic surge (for example electrocardiograms) experimented at 125 Hz, collected commencing male and female grown-up

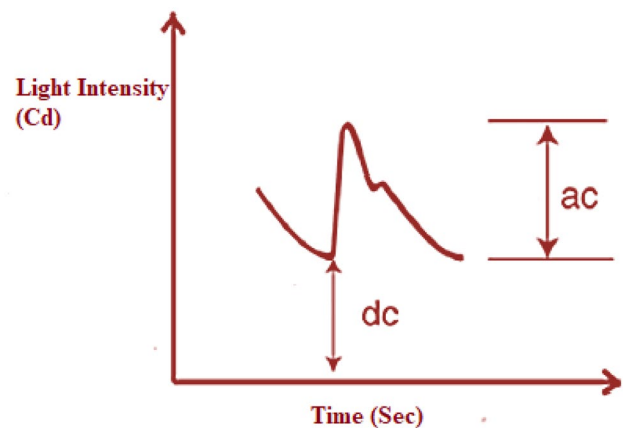


Fig. 1 PPG wave along with its DC and AC constituents

subjects aged 21 to 90 with a variety of pathologies including pulmonary illness.

The subsequent section provides an outline for the remaining content of the paper. In part 2 of the document, you will find a brief description of the related work. This section provides an overview of the existing research and studies that are relevant to the topic at hand. Moving on to Sect. “[The Objective of the research](#)”, you will find a detailed explanation of the methodology employed in this study, as well as the theoretical foundations that underpin the methods used. This section aims to provide a clear understanding of the approach taken and the principles guiding the research process. In Sect. “[Proposed Algorithm](#)”, we will discuss the simulation results and analysis. In the concluding section of this research paper, titled “key findings,” we aim to provide a concise summary of the most significant outcomes.

## Existing Methodology

For arterial pressure readings and pulse oximetry (SpO<sub>2</sub>/PPG) signals, developed an automatic systolic peak recognition system that identifies the first peak after each heartbeat. Incorporating a filter bank with tunable cut-off frequencies, rank-order nonlinear filters, spectral estimations of heart rate, and a decision-making framework [16]. However, the computational inefficiency comes from the fact that the decision logic discards all candidate components if the temporal constraints are not met [17].

It was suggested by that an automatic delineator may be used to locate fiducial spots on the waveform of arterial blood pressure, such as onsets, systolic peaks, and diastolic notches. The delineator is based on the combinatorial analysis of the original waveforms and their first-order derivatives [18], and additional decision logics were introduced in order to deal with pathologic complexity, instrumental unreliability, and the final selection of probable diastolic notches. Since this method only takes into account derivatives of the first order, it is possible that it will not be able to correctly comprehend the waveform that was first given. In addition, when it is not there, the delineator fixes an empirical point as the diastolic notch in a third of the temporary searching window. This point can subsequently be adjusted [19].

A detection method that compares the fit of broken-stick and straight-line models within a sliding time window was suggested [20] as a means of locating the onset, systolic peak, diastolic notch, and diastolic peak in the PPG waveform. This would allow for the identification of these elements. The proposed method has a pretty low level of accuracy when it comes to producing accurate detections, which is something that might be improved.

A method for detecting the systolic peak was developed, and it was based on local maxima-minima, first-derivative, and slope sum. This was done so that the detection rate could be increased. The advantage of the proposed method is that it eliminates the requirement for human input in selecting where to set the threshold [21]. This is an important advantage. Because of this, it is an excellent choice for applications that take place in real time. Even though it has presented certain PPG morphologies, that does not mean that it has presented all of them [1].

To find the systolic peaks, suggested a method that uses a moving average of valley-peak differences in conjunction with an adaptive threshold filtering. When the threshold coefficient is lowered, there is a greater likelihood of false positives [22].

In order to create a binary classifier, [23] devised an algorithm that uses the notion of threshold comparison between the consecutive samples to recognise the peak and foot fiducial points in PPG and the diastolic notch and diastolic peak in SDPPG. With this method, we can detect fiducials with a high degree of accuracy.

To avoid the need for any preliminary processing of PPG waveforms, [24] created a peak identification system based on an adaptive segmentation method (ASM). Subjects with different pathophysiological difficulties were not evaluated, and the study only included 20 healthy volunteers who had no history of cardiovascular, neurological, or respiratory problems.

Using a topological signal processing framework, authors suggested a unique method based on persistence intervals for extracting the systolic peak, anacrotic notch, diastolic notch, and diastolic foot of pulse pressure waves [25]. Twenty-eight participants' radial pressure pulses were collected using a wearable tonometer to further validate this method. The researchers then calculated the peripheral augmentation index using both the derivative and persistence based methods and found no significant differences between them.

In [26] studied 112 pregnant and nonpregnant persons of varying ages to determine the repeatability of arterial stiffness parameters evaluated by digital pulse wave analysis (DPA) and the connections to applanation tonometry parameters. With respect to the ejection elasticity index (EEI), the age index (AI), and the b/a, the associations were all stronger with AIx than with PWV. They concluded that the EEI, AI, and b/a were the most effective DPA parameters.

Twenty intensive care unit (ICU) patients' PRV and HRV were analysed using multiscale entropy (MSE) to determine if PRV might replace HRV. Using Poincare plots, they also linked PRV from four PPG-based approaches to HRV from the gold-standard R-R interval method [27]. They found that no PPG-based method

correlated or agreed well enough with the gold-standard ECG-based method, leading them to the conclusion that PRV might not be a practical option for estimating MSE values and Poincare plots of HRV.

Using photoplethysmography (PPG), investigators [28] proposed iPRV as a surrogate for Heart Rate Variability (HRV) and Pulse Rate Variability (PRV) in non-stationary conditions. Researchers analysed the iPRV and HRV of 24 subjects during a passive leg raise (PLR) experiment in time-domain and discovered a favourable correlation between the two ( $r$ -value = 0.6800.099 at baseline and  $r$ -value = 0.6880.096 during PLR). They also suggested that time-domain PPG analysis is a better diagnostic for clinical use.

Researchers looked at the viability of HRV indices derived from finger PPG as a potential replacement for HRV derived from ECG signal. Thirty-three people participated in the study, and their PPG and ECG signals were captured at the same time under both resting and exercise situations. Mean and standard deviation (SDNN) of intervals over 5 min were calculated from PPG and ECG waveforms, and the PPG and ECG PPI and RRI were determined for each condition. They found that the PPI and RRI have a stronger cross correlation when at rest than when exercising, indicating that the HRV indices can be reliably evaluated from PPG when at rest.

## The Objective of the Research

To better diagnose cardiovascular evaluations, this publication proposes an effective approach for adaptive IoT based delineation of PPG waveforms. Specifically, this study aims to:

- Improve diagnosis with your new, more powerful method for segmenting PPG waveforms based on their second-order derivative. You can evaluate arterial stiffness by using the proposed technique to analyse physiological features gleaned from the PPG signal.
- Photoplethysmographic augmentation index (PAI) for arterial stiffness estimation and demonstrating PAI's correlation with CVD risk in clinical research.

## Proposed Algorithm

Subsequently most delineation methods rely on the size of the temporary searching window employed or thresholding, the size of these windows and thresholds must be calculated empirically, and in the absence of a fiducial point, such as a dicrotic notch, a fiducial point

must be set experimentally. If these criteria are not chosen properly, the algorithm's overall performance could suffer. Some algorithms to generate blocks of interest, with the unwanted blocks being filtered out in the process, use two moving average filters, then a dynamic event length threshold. For this reason, an optimised algorithm is required to guarantee the existence of representative points in all of its recurrences and to improve performance in relations of sensitivity besides great optimistic predictivity. The resampling approach can be used to do this. Therefore, it is proposed to develop an algorithm in Matlab to outline the important facts of PPG data with numerous pathophysiological impediment, found from the high-gauge acquiescently obtainable data record from PhysioNet, while also guaranteeing the existence of representative facts in altogether its recurrences through a sampling method again.

## BPF Filtering

It is common for aliasing points to be introduced in derivatives of raw PPG unprocessed waveforms due to the presence of numerous sounds and artefacts. When the PPG signal and its derivatives are evaluated using an algorithmic strategy, these confounding variables may impair feature extraction and, by extension, the accuracy of the diagnosis. Noise and artefacts in the original PPG signals can typically be reduced using Band Pass Filters (BPF).

It is crucial to condition the signal using effective digital filtering that takes into account baseline drift in addition to additional squat and great frequency constituents. Maximum of the vitality of the PPG data is less than 9 Hz, therefore we can filter out the great-frequency clamour that subsists beyond 9 Hz and the small-frequency clamour that origins reference line drifting in the range of 0.5 Hz by employing Fast Fourier Transform (FFT). It is at these lower frequencies that the signal appears to be least filtered. Figures 2, 3, 4, 5 depicts the raw signal's spectrum as well as its filtered signal, making it evident that the filtered signal lacks the unwanted spectrum [28].

## 2nd Derived Evaluation

First, second, and fourth order derivatives identify phase shifts in the original PPG waveform. SDPPG, or acceleration plethysmogram, is often utilized over the first derivative because it allows for easier understanding of the original waveform. It has five successive waves termed a, b, c, and d waves in the systolic stage and e wave signifying the dicrotic slash in the diastolic stage. Various articles have statistically evaluated the relationship between cardiovascular risk

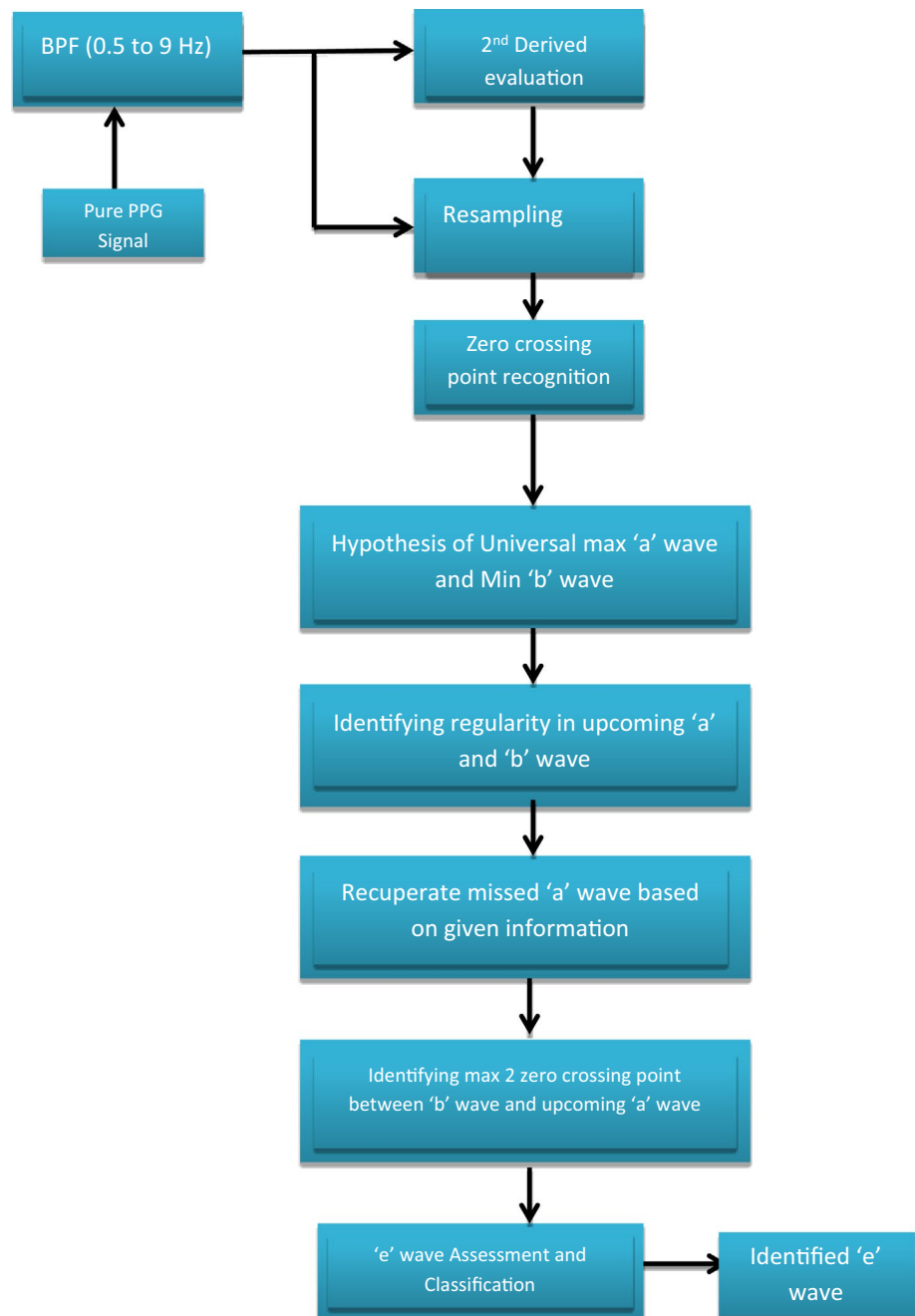
variables and SDPPG normalized amplitudes. Most cardiovascular diseases are determined from a, b, and e waves.

Though the experimental consequences of SDPPG extent have been described in length, investigations concentrating on the programmed recognition of this information in SDPPG data are needed to communicate cardiac healthiness.

### Signal Re-Sampling

The PPG signal is used to implement the segmentation into a single beat through situation to the ECG explanation in the data record, and ECG data are applied to authenticate the beat recognition. The beat-by-beat performance evaluations are validated against the corrective reference provided by the approved ECG annotations in the database. In other words, visual inspection was used to determine the state of delineator findings. A weary recognition is classified as either correct optimistic or incorrect adverse grounded on

**Fig. 2** The Proposed Method Block Diagram



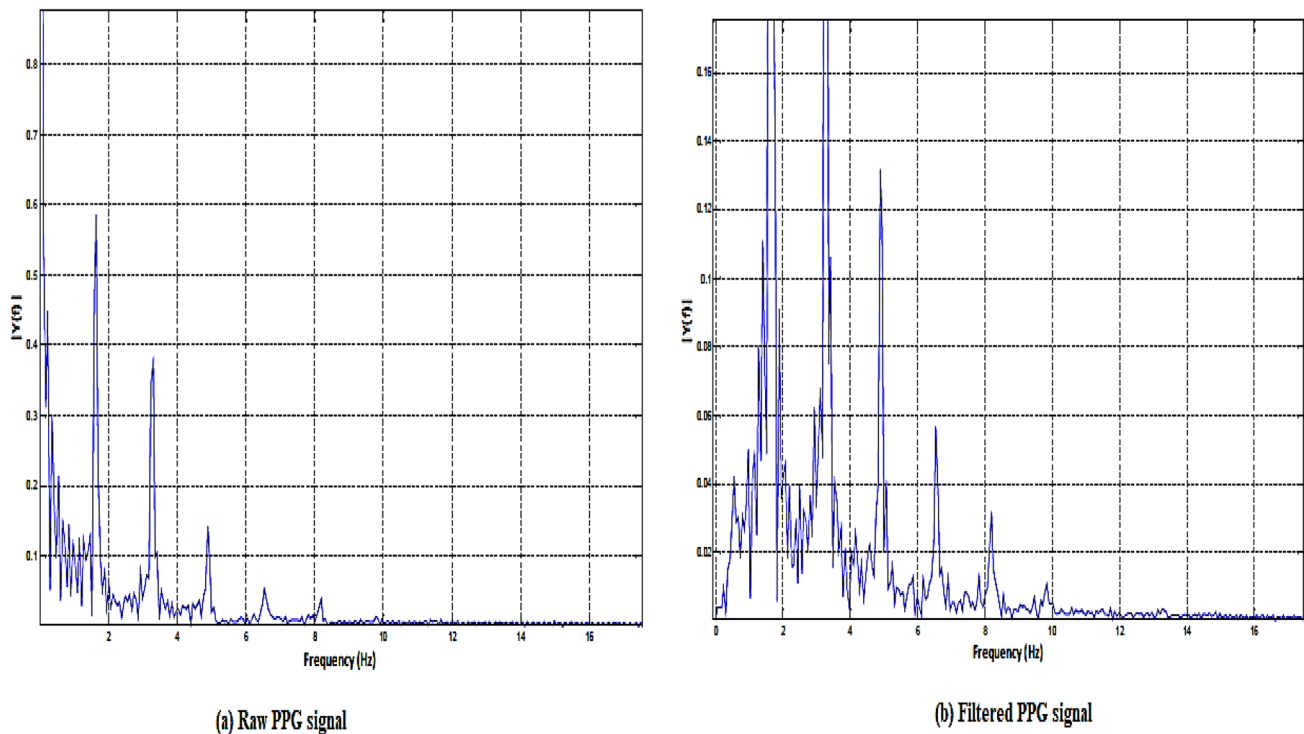


**Fig. 3** Spectrum of PPG signals (a) Untainted PPG data (b) Eviscerated PPG data

the occurrence or absenteeism of a distinct PPG waveform and accompanying ECG annotation. If the PPG waveform is ambiguous or the ECG is unannotated, the result is classified as a false positive (FP).

Additionally, bio-signals associated with cardiac activity are non-periodic but recurrent; for example, the choral constituents of two successive reappearances of the PPG data and its offshoots may have diverse frequencies. The repetitions are defined as the time between successive peaks in the signal. To ensure that all harmonic components are treated in the same manner, we first resample the SDPPG signal to equalise the lengths of the recurrences, as described in the algorithm below. Re-sampling the SDPPG signal ensures that each repetition will have the same figure of sections in an affecting space. The PPG signal is divided into sub-signals of a predetermined repetition rate. Each chosen repetition of the PPG signal is sampled again using the similar numeral of models and then associated with the others. After that, we take an average across each period's  $M^{\text{th}}$  sample. For the SDPPG signal, we used the same procedure.

### Feature Abstraction and Ordering

When drawing the SDPPG, the delineator looks for all the beats where the zero-crossing points are positive. The PPG waveforms are then analysed, and the candidate onsets

and systolic peaks are scored based on the validated ECG annotations in this database. After identifying synchronization through all supplementary utmost facts, the delineator treats the universal extreme fact as a surge in every weary. Using a fixed point on the SDPPG signal as a point of reference, like the wave's maximum recurrence point, allows for coordinated zero-crossing sites. After analysing 46 separate records, we find that the middling bounty of the "a" surge in every dataset is amongst 0.0152 and 0.052, with a variance of 0.005. If a fact is missing during some stretch period, the delineator will use the middling bounty and deviance of 0.006 between the leading and last beats to try to find it again and recover it. The algorithm identifies the first minimum value that occurs following an a-wave as the b-wave, and it then correlates this value with the subsequent minimum values. Since a dicrotic notch is expected to appear between the b wave and the subsequent onset, the given delineator can also pinpoint the position of the e wave inside that interval (a wave). After identifying a and b waves, we identify the e wave (dicrotic notch) as the optimistic zero-intersection fact through the highest uttermost amongst the current b surge and the following a surge, provided that this point does not deviate over the course of a single beat. The e waves are classified through optimistic discrete wavelet and CNN based approach.

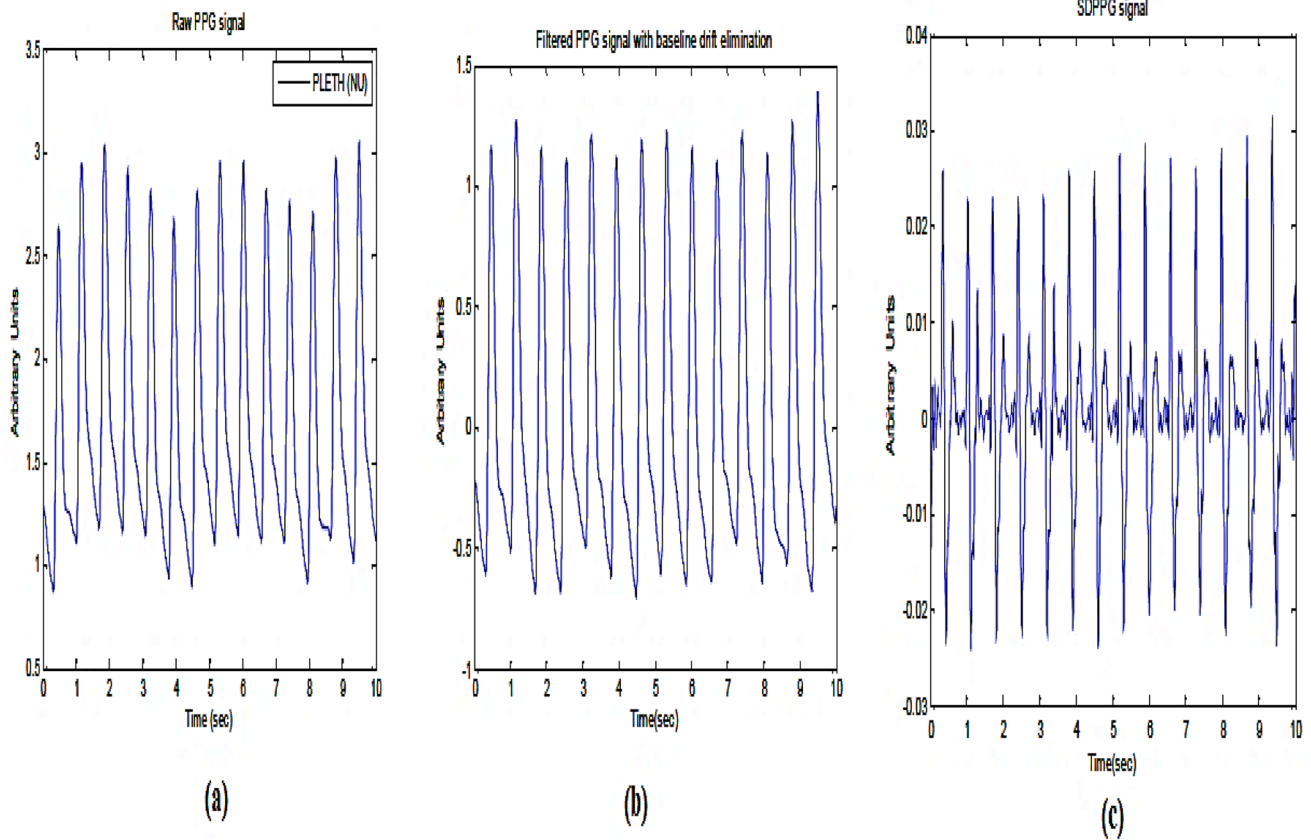


Fig. 4 The Projected Filtered Output (a) Pure PPG untreated data (b) Cleaned PPG data with baseline theme removal (c) SDPPG data

### Performance Assessment

To evaluate the effectiveness of the provided delineator, we estimate common statistical parameters: Accuracy, Sensitivity (Se) and Specificity as formulated below.

$$\text{Accuracy} = \frac{\text{TN} + \text{TP}}{\text{Total data Sample}} \times 100 \tag{1}$$

$$\text{Sensitivity} = \frac{\text{TN}}{\text{TN} + \text{FP}} \times 100 \tag{2}$$

$$\text{Specificity} = \frac{\text{TN}}{\text{TN} + \text{FP}} \times 100 \tag{3}$$

True positives (TP) are the number of times an a/b/e wave was correctly identified as an a/b/e wave; false negatives (FN) are the number of times an a/b/e wave was incorrectly

identified as not being present; and false positives (FP) is the number of times an incorrect wave type was incorrectly identified as present. For the selected records, we calculate an overall performance rating for the accuracy with which they recognise both the beginning (a surge) and the b surge in PPG waves. The results of the IoT based delineator were evaluated visually, and both a and b waves were taken into account. A beat was classified as “TP” if the PPG waveform could be clearly seen, “FN” if it could not, and “FP” if it was barely detectable.

### Result and Discussion

To confirm the delineator as True Positive or reject it as False Positive or FN aimed at a surge, for instance, all global maximum peaks with moving point coordination were

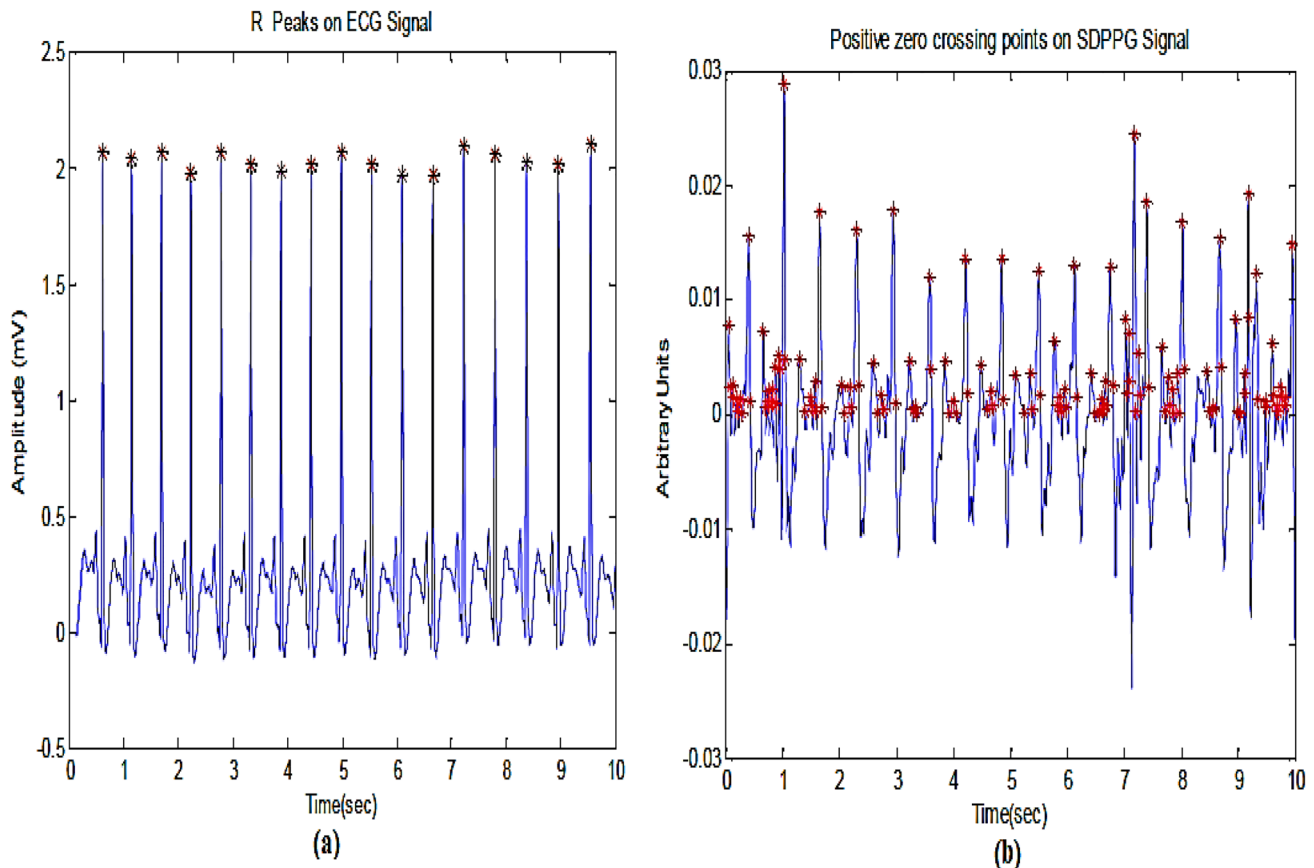


**Fig. 5** Stages Convolved in the Recognition of a, b and e Surges **(a)** R crests on ECG data **(b)** Optimistic zero intersections on SDPPG data

selected (onset). Since a waves tend to have comparable amplitudes, the delineator was able to account for their sharp peaks (high amplitude) and the statistical characteristics of the signals (i.e., mean and standard deviation) do not change much over time. The b wave follows the a wave and is the principal least afterwards the a surge regardless of either it is a universal least or a confined least in subjects through worthy or deprived transmission. The delineator classifies as b waves all the first minimum points that follow a wave and are coordinated by moving points. For following pulse contour analysis during IoT based PPG characterization, the delineator results are more trustworthy than those from thresholding techniques.

The steady heartbeat is examined through affluence, since 'a' surges are uniformly spread out and consequently the occurrence of the succeeding weary is expectable. An asymmetrical heartbeat is often connected to whichever premature thumps and the projected outlier efficiently detect a surges in an asymmetrical data which furthermore associates to 16 strokes in ECG II prime for this recording in the data. The suggested outlier furthermore recognises a influences exactly even in inconsistent amplitude non-static PPG data. This record's average a-wave amplitude is 0.02,

however due to a discrepancy of 0.005, the a-wave recorded at 0.014 is FN. Equating the PPGs of 28 fit young helpers to the PPGs of ill patients and the elderly, it is evident that the suggested outlier is additional amplitude-liberated. The enactment of the b surge recognition reached virtually the identical outcome as detection, as the recognition of b surge determined by on the recognition of a surge. With no false positives, the suggested a and b detection achieved a 99.89% optimistic predictivity besides a 99.96% sensitivity, demonstrating the stability of the delineator. The outlier informed 2 FNs and 1 FP, resulting to the enactment keys of e wave recognition with Se (98.89 percent).

Table 1 and Fig. 6 provides a comparison of the proposed method's performance to that of several other methods based on machine learning. With an accuracy of 99.7%, Sensitivity of 96.2%, and specificity of 99.9% for Normal pulses wavelet-based CNN with PPG signal provides superior classification results.

Table 2 and Fig. 7 present a comparison of the performance of the proposed technique to that of a number of different methods that are based on machine learning. Wavelet-based CNN combined with PPG signals produce superior

classification results, with an accuracy of 99.8%, sensitivity of 99.8%, and specificity of 96.5% for P1 pulses respectively.

The performance of the suggested method is compared in Table 3 and Fig. 8 to the performance of numerous other methods that are based on machine learning. Wavelet-based CNN combined with PPG signals produce superior classification results, with an accuracy of 99.8%, sensitivity

of 99.8%, and specificity of 95.7% for P2 pulses respectively (Fig. 9).

Due to strong motion distortions, the classification accuracy of the P2 pulse dropped as a result of misclassification with several smaller pulses. The multiscale frequency information related to premature pulses might be obtained at each node of the provided signal with the help of the discrete wavelet transform. The features extracted by CNN aid the proper classification of e pulses. Our approach should not miss any pulses because it estimates the wavelet transform on a signal's entire duration every second. Increases in sensitivity and specificity can also be achieved through incremental fine-tuning of CNN. When compared to other state-of-the-art methods, the wavelet-based CNN improves the accuracy, sensitivity, and specificity of e-wave classification.

**Table 1** Normal pulse classification performance analysis of proposed discrete wavelet based CNN method with other state-of-art methods

| S. no | Classifiers                               | Accuracy (%) | Specificity (%) | Sensitivity (%) |
|-------|---|--------------|-----------------|-----------------|
| 1.    | SVM [19]                                  | 91.2         | 92.6            | 88.1            |
| 2.    | KNN [29]                                  | 95.8         | 99.9            | 89.2            |
| 3.    | Morphological features + ANN [17]         | 99.5         | 94.3            | 99.5            |
| 4.    | Proposed discrete wavelet transform + CNN | 99.7         | 96.2            | 99.9            |

### Conclusion and Future Scope

An Internet of Things grounded PPG waveform delineator is projected and implemented in this research publication in order to report on the commencements of a surge, b surge, and e surge that are enumerated by SDPPG. Numerous delimiters conducted research on performance evaluation,

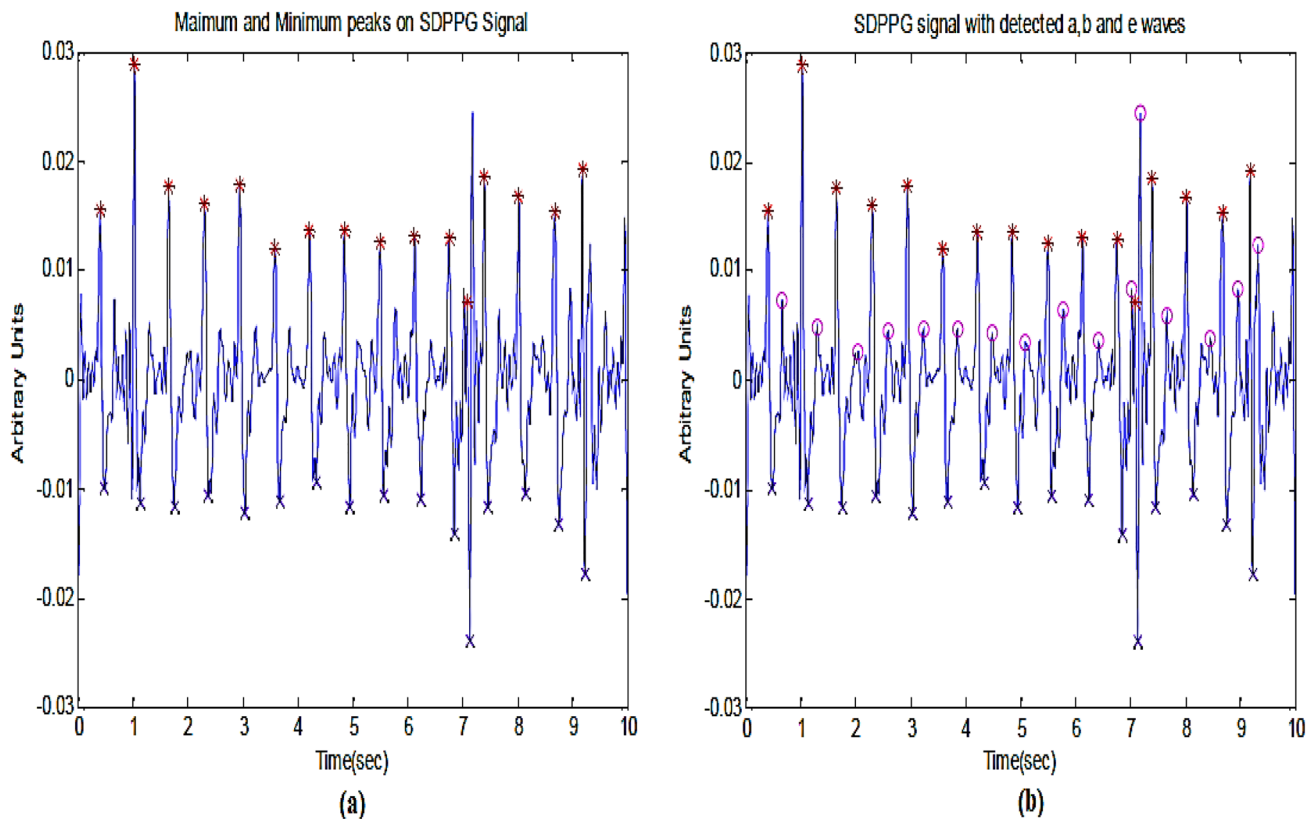


**Fig. 6** Stages Convolved in the Recognition of a,b and e Surges (a) Extreme and lowest crests on SDPPG data (b) Recognition of a (star), b (cross) besides e (circle) surges

**Table 2** P1 pulse classification performance analysis of proposed discrete wavelet based CNN method with other state-of-art methods

| S. no. | Classifiers                               | Accuracy (%) | Specificity (%) | Sensitivity (%) |
|--------|---|--------------|-----------------|-----------------|
| 1.     | SVM [19]                                  | 94.6         | 95.8            | 89.8            |
| 2.     | KNN [29]                                  | 96.2         | 96.4            | 92.7            |
| 3.     | Morphological features + ANN [17]         | 99.4         | 99.6            | 95.3            |
| 4.     | Proposed discrete wavelet transform + CNN | 99.8         | 99.8            | 96.5            |

but their studies were restricted to either small datasets or a subset of patients. The existing proposed method was only subjected to testing on healthy young adults, hence its robustness has not been confirmed in unhealthy patients. The suggested delineator is evaluated on PPG signals from a variety of patient populations, including healthy adults, sick patients, and the elderly, and is shown to be more amplitude-independent than the delineator developed using PPGs from 28 young, healthy volunteers. In addition, resampling the SDPPG signal ensures the occurrence of particular facts when it comes to the process of building slabs of attention, in which the undesired slabs are primarily removed by means of onset criteria. Research provides a comparison of the performance of the proposed method to that of other machine learning based techniques. In terms of classification accuracy (Normal, P1, and P2 pulses: 95.9%, 93.4%, and 90.08% respectively), wavelet-based CNN with PPG signal outperforms CNN with PPG and ABP signals. Misclassification with certain smaller pulses occurred, lowering the classified accuracy of P2 pulse

due to strong motion artifacts. The multiscale frequency information at each location of the provided signal related to premature pulses could be obtained using the discrete wavelet transform. Correct classification is aided by CNN's ability to extract many features associated with premature pulses. To ensure that no pulses are missed, our method estimates the wavelet transform at one-second intervals over the whole signal's duration. CNN's incremental fine tuning also aids in improving both sensitivity and specificity. The wavelet-based CNN outperforms other state-of-the-art approaches in terms of accuracy, sensitivity, and specificity when classifying waves.

It felt very ironic that the substantial amount of PPG data that was used in the performance evaluation. However, in order to validate these results, we require further data gathered from a larger pool of subjects. Additionally, a more sensitive e-wave detector requires a higher sample rate for PPG signals in order to function properly.

**Table 3** P2 pulse classification performance analysis of proposed discrete wavelet based CNN method with other state-of-art methods

| S. no. | Classifiers                               | Accuracy (%) | Specificity (%) | Sensitivity (%) |
|--------|---|--------------|-----------------|-----------------|
| 1.     | SVM [19]                                  | 94.8         | 96.7            | 90.7            |
| 2.     | KNN [29]                                  | 95.4         | 97.3            | 91.2            |
| 3.     | Morphological features + ANN [17]         | 99.7         | 99.8            | 94.2            |
| 4.     | Proposed discrete wavelet transform + CNN | 99.8         | 99.8            | 95.7            |

**Fig. 7** Normal Pulse Classification Performance analysis of proposed discrete wavelet based CNN method with other state-of-art methods

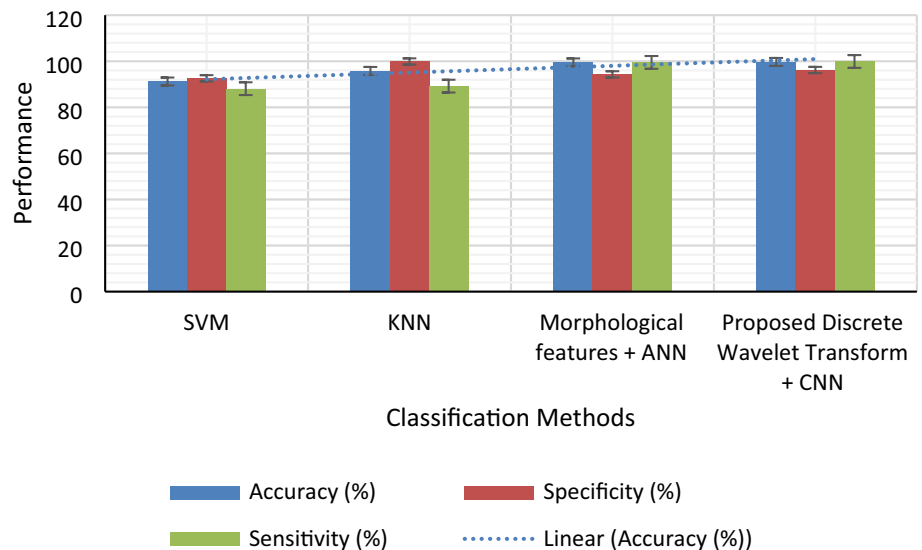


**Fig. 8** P1 Pulse Classification Performance analysis of proposed discrete wavelet based CNN method with other state-of-art methods

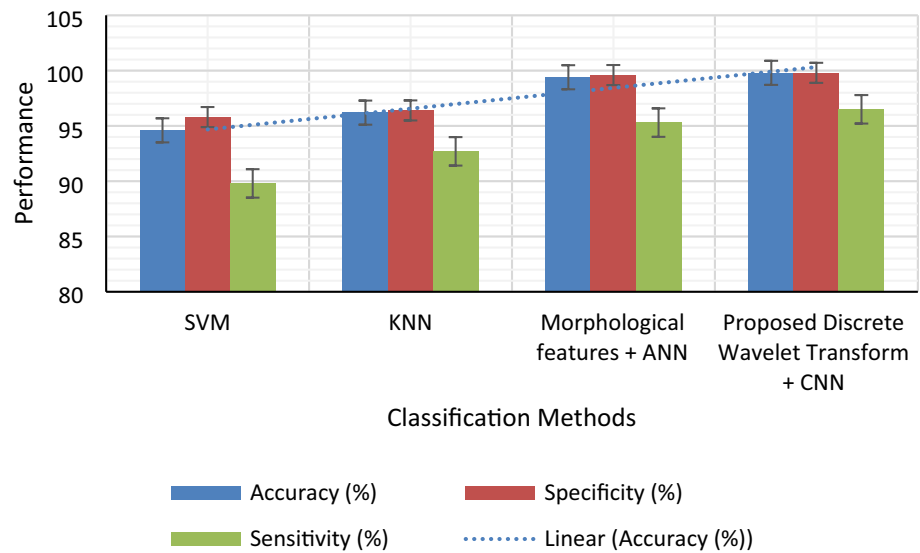
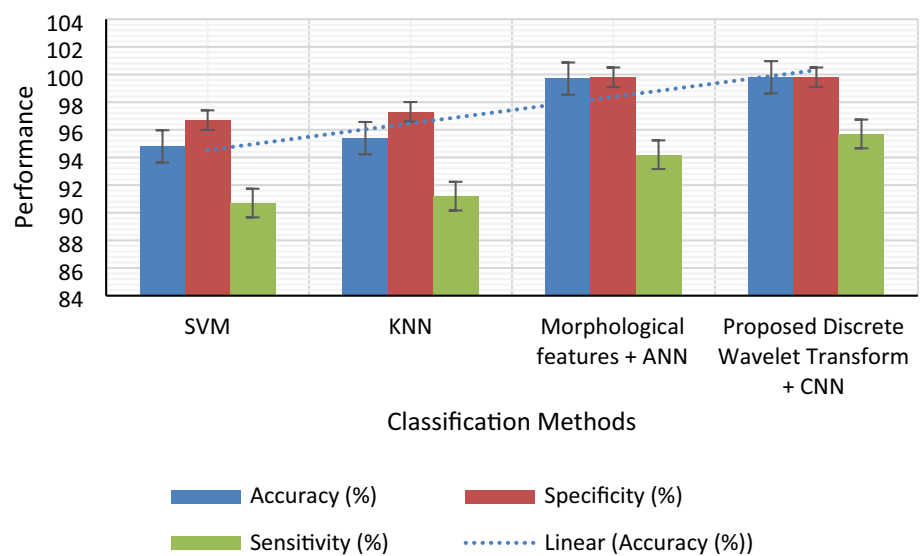


**Fig. 9** P2 Pulse Classification Performance analysis of proposed discrete wavelet based CNN method with other state-of-art methods



**Data Availability** Data sharing is not applicable to this article as no datasets were generated or analysed during the current study.

**Declarations**

**Conflict of Interest** The authors declare no conflict of interest.

**Ethical Approval** This article does not contain any studies with animals performed by any of the authors.

**References**

- Resit A, Kavsaoglu K, Polat MR. An innovative peak detection algorithm for photoplethysmography signals: an adaptive segmentation method. *Turkish J Electr Eng Comp Sci.* 2016;24:1782–96.
- Arrozaq A, Hamdan F, Rhandy A, Hasballah Z. Early detection of cardiovascular disease with photoplethysmogram (PPG) sensor, *Proceedings of the International Conference on Electrical Engineering and Informatics (ICEEI).* 2015
- Elgendi M. Detection of c, d, and e waves in the acceleration Photoplethysmogram. *Comput Methods Programs Biomed.* 2014;117:125–36.
- Narayana D, Shruthi, S Digital processing of ECG and PPG signals for study of arterial parameters for cardiovascular risk assessment, *Proceedings of the International Conference on Communications and Signal Processing,* 2015, 1506–1510
- Parasnis R, Pawar A, Manivannan, M. Multiscale entropy and poincare plot-based analysis of pulse rate variability and heart rate variability of ICU patients, *Proceedings of the International Conference on Intelligent Informatics and Biomedical Sciences,* 2015, pp. 290–295.
- Shukla S, Roy V, Prakash A. Wavelet based empirical approach to mitigate the effect of motion artifacts from EEG Signal, 2020

- IEEE 9th International Conference on Communication Systems and Network Technologies (CSNT), 2020, pp. 323–326, doi: <https://doi.org/10.1109/CSNT48778.2020.9115761>.
7. Kudo S, Chen Z, Zhou X, Izu L, Chen-Izu Y, Zhu X, Tamura T, Kanaya S, Huang M. A training pipeline of an arrhythmia classifier for atrial fibrillation detection using Photoplethysmography signal. *Front Physiol.* 2023;14:2.
  8. Senghiphany, T, Tretriluxana, S, Chitsakul, K. Comparison of Heart Rate statistical parameters from Photoplethysmographic signal in resting and exercise conditions, Proceedings of the 12th International Conference on Electrical Engineering/ Electronics, Computer, Telecommunications and Information Technology, 2015, pp. 766–770.
  9. Shadi, SC, Belhage B, Hoppe K, Branbjerg J, Thomsen EV. Sternal pulse rate variability compared with heart rate variability on healthy subjects, Proceedings of the 36<sup>th</sup> Annual International Conference of the IEEE Engineering in Medicine and Biology Society, 2014, pp. 3394–3397.
  10. Kuntamalla S, Ram Gopal Reddy L. An efficient and automatic systolic peak detection algorithm for photoplethysmographic signals. *Int J Comp Appl.* 2014;97(19):18–23.
  11. Talukdar D, Deus L, Sehgal N. Evaluation of atrial fibrillation detection in short-term photoplethysmography (PPG) signals using artificial intelligence. *MedRxiv.* 2023;2023:23286847.
  12. Chen C, Hua Z, Zhang R, Liu G, Wen W. Automated arrhythmia classification based on a combination network of CNN and LSTM. *Biomed Signal Process Control.* 2020;57: 101819.
  13. Emma W, Östling G, Nilsson PM, Olofsson P. Digital photoplethysmography for assessment of arterial stiffness: repeatability and comparison with applanation tonometry. *PLoS ONE.* 2015;10:19.
  14. Roy V, Shukla S. Designing efficient blind source separation methods for EEG motion artifact removal based on statistical evaluation. *Wireless Pers Commun.* 2019;108:1311–27. <https://doi.org/10.1007/s11277-019-06470-3>.
  15. Panwar M, Gautam A, Biswas D, Acharyya A. PP-Net: A deep learning framework for PPG-based blood pressure and heart rate estimation. *IEEE Sens J.* 2020;20:10000–11.
  16. Aschbacher K, Yilmaz D, Kerem Y, Crawford S, Benaron D, Liu J, Eaton M, Tison G, Olgin J, Li Y, et al. Atrial fibrillation detection from raw photoplethysmography waveforms: a deep learning application. *Heart Rhythm.* 2020;O2(1):3–9.
  17. Ghosal P., Rajarshi G. Classification of photoplethysmogram signal using self organizing map, Proceedings of the IEEE International Conference on Research in Computational Intelligence and Communication Networks, 2015, pp. 114–118.
  18. Ivrea D, Veiga C, Rodríguez-Andina J, Farña J, Garcixa E. Using support vector machines for atrial fibrillation screening. In Proceedings of the 2017 IEEE 26th International Symposium on Industrial Electronics (ISIE), Edinburgh, UK, 19–21 June 2017; pp. 2056–2060.
  19. Roy V, Shukla S. Effective EEG motion artifacts elimination based on comparative interpolation analysis. *Wireless Pers Commun.* 2017;97:6441–51. <https://doi.org/10.1007/s11277-017-4846-3>.
  20. Mohamed E, Ian N, Matt B, Derek A, Dale S. Detection of a and b waves in the acceleration photoplethysmogram. *Biomed Eng Online.* 2014;13:139–56.
  21. Elgendi M, Norton I, Brearley M. Systolic peak detection in acceleration photoplethysmograms measured from emergency responders in tropical conditions. *PLoS ONE.* 2013;8(10):1–11.
  22. El-Hajj C, Kyriacou P. A review of machine learning techniques in photoplethysmography for the non-invasive cuff-less measurement of blood pressure. *Biomed Signal Process Control.* 2020;58: 101870.
  23. Blazek R, Lee C. Multi-resolution linear model comparison for detection of dicrotic notch and peak in blood volume pulse signals, Proceedings of the International Biosignal Processing Conference: Biosignal, 2010, pp. 378–386.
  24. Khandoker AH, Karmakar CK, Palaniswami M. Comparison of pulse rate variability with heart rate variability during obstructive sleep apnea. *J Med Eng Phys.* 2011;33(2):204–9.
  25. Shukla S, Roy V, Prakash A. Wavelet based empirical approach to mitigate the effect of motion artifacts from EEG signal, 2020 IEEE 9th International Conference on Communication Systems and Network Technologies (CSNT), Gwalior, India, 2020, pp. 323–326, doi: <https://doi.org/10.1109/CSNT48778.2020.9115761>.
  26. Loh H, Xu S, Faust O, Ooi C, Barua P, Chakraborty S, Tan R, Molinari F, Acharya U. Application of photoplethysmography signals for healthcare systems: An in-depth review. *Comput Methods Biomed.* 2022;216: 106677.
  27. Soundararajan M, Arunagiri S, Alagala S. An adaptive delineator for photoplethysmography waveforms. *Biomed Eng.* 2016. <https://doi.org/10.1515/bmt-2015-0190>.
  28. Zhang Y, Zhang Y, Siddiqui S, Kos A. Non-invasive blood-glucose estimation using smartphone PPG signals and subspace kNN classifier. *Elektrotehniski Vestn.* 2019;86:68–74.

**Publisher's Note** Springer Nature remains neutral with regard to jurisdictional claims in published maps and institutional affiliations.

Springer Nature or its licensor (e.g. a society or other partner) holds exclusive rights to this article under a publishing agreement with the author(s) or other rightsholder(s); author self-archiving of the accepted manuscript version of this article is solely governed by the terms of such publishing agreement and applicable law.

## Authors and Affiliations

Srinivasa Rao Sankranti<sup>1</sup>  · S. Mahaboob Basha<sup>2</sup>  · B. Laxmi Kantha<sup>3</sup>  · L. Bhagyalakshmi<sup>4</sup>  · N. Gomathi<sup>5</sup>  · Kuchipudi Prasanth Kumar<sup>6</sup>  · Sanjay Kumar Suman<sup>7</sup> 

✉ L. Bhagyalakshmi  
Prof.Dr.L.Bhagyalakshmi@gmail.com

Srinivasa Rao Sankranti  
ssankran@gitam.edu

S. Mahaboob Basha  
mahaboobshas.sse@saveetha.com

B. Laxmi Kantha  
kanthis.chinnu@gmail.com

N. Gomathi  
gomathin@veltech.edu.in

Kuchipudi Prasanth Kumar  
kprashanth510@gmail.com

Sanjay Kumar Suman  
Prof.dr.sanjaykumarsuman@gmail.com

- <sup>1</sup> Department of EECE, GITAM Deemed to be University, Rushikonda, Visakhapatnam, AP, India
- <sup>2</sup> Department of CSE, Saveetha School of Engineering, Saveetha Institute of Medical and Technical Sciences, Saveetha University, Chennai, TN, India
- <sup>3</sup> Department of IT, St. Martin's Engineering College, Secunderabad, Telangana, India

- <sup>4</sup> Department of ECE, Rajalakshmi Engineering College, Chennai, TN, India
- <sup>5</sup> Department of CSE, Veltech Rangarajan Dr.Sagunthala R&D Institute of Science and Technology, Chennai, TN, India
- <sup>6</sup> Department of Computer Science and Engineering, Koneru Lakshmaiah Education Foundation, Vaddeswaram, Guntur, AP, India
- <sup>7</sup> Department of ECE, and Dean R&D, St. Martin's Engineering College, Secunderabad, Telangana, India